SENSOR LETTERS
Vol. 11, 2038–2042, 2013

RESEARCH ARTICLE

Gold Nanoparticle Embedded Titanium Dioxide Thin Film for Surface Plasmon Resonance Gas Sensing at Room Temperature

Gaige Zheng*, Linhua Xu, Yu Zhan, Yigen Wu, and Chengyi Zhang

School of Physics and Optoelectronic Engineering, Nanjing University of Information Science and Technology, Nanjing 210044, China

(Received: 14 November 2012. Accepted: 19 June 2013)

The optical gas sensing properties of gold (Au) nanoparticles (NPs) doped into titanium dioxide (TiO_2) matrix prepared by sol–gel method and annealed at different temperatures have been investigated. AFM images reveal that the Au NPs are exuded from the film during annealing. The chemical interaction of the hydrogen (H_2) and carbon monoxide (CO) molecules on the Au surface will increase the overall electron concentration on the metal side, cause a decrease in Au metal bulk plasma wavelength, and the surface plasmon resonance (SPR) peak can be used for the realization of a gas sensor with tunable sensitivity. The plasmonic responses are observed to be sensitive toward the presence of target gases. The results reveal that on decorating the Au NPs at the room temperature gas adsorption can be made possible due to the presence of Au NPs. We estimate that this kind of Au-NPs embedded in TiO_2 film can be a promising material for nanophotonic and electrochemical sensor applications.

Keywords: Titanium Dioxide Thin Film, Surface Plasmon Resonance, Gas Sensor, Gold Nanoparticle, Sol–Gel Method.

1. INTRODUCTION

Surface plasmon resonance (SPR) is an optical effect caused by the interaction of the surface plasmon (SP) with the incident electromagnetic radiation at a resonant frequency.[1,2] Metals exhibit plasmon effect because they have a high density of free electrons. The sensitivity of the plasmon depends on particle size, shape, the refractive index of the medium and the dielectric constants of the metal. The excitation of SP by light is sometimes denoted as a localized surface plasmon resonance (LSPR) for the nanoscale metallic systems,[3] this phenomenon occurs due to the local field around the particles which cause the modification in their dielectric function. The response of the NPs present in the medium can be described by Maxwell-Garnett dielectric function[4] and could show catalytic properties therefore modify the chemical interactions between the oxide surface and the target analyte, improving the sensing process.[5] Moreover, if the metal NPs show LSPR peak in the visible range, the nanocomposites can be used as selective optical gas sensor.[6] Gold (Au) is the promising candidate due to its excellent surface properties and the advantages include non-toxicity, strong scattering length, bio-conjugation and long-term stability which are essential for a stable and sensitive sensing platform. With the incorporation of a host-matrix thin film, the hybrid materials represent an attractive solution to many present and future technological demands because they combine the promising optical properties of NPs with those of the host matrix.[7–9] Recently, highly dispersed noble metal NPs with desirable morphologies have attracted great attention due to their unusual catalytic, electric, optical properties and SP absorption, and their widespread potential usefulness in diverse fields such as biomedicine, photocatalysis, energy conversion, and storage and nanodevices.[10,11]

Titanium dioxide (TiO_2) is a non-toxic material and the thin films exhibit high stability in aqueous solutions and no photocorrosion under band gap illumination and special surface properties. TiO_2 is the subject of intensive research, especially with regard to its uses in solar cells, chemical sensors, electronic devices and so on.[12–15] Au NPs supported on TiO_2 surfaces show surprisingly high chemical activity and have attracted considerable attention,

*Corresponding author; E-mail: eriot@126.com

1546-198X/2013/11/2038/005 doi:10.1166/sl.2013.3056

both for fundamental and applications reasons.[15–19] The optical properties of nanocrystal-doped thin films are dominated in the visible range by the SPR of the noble metal NPs.

An important problem that prevents the development of further applications of such plasmonic nanocomposite films is the lack of a reliable, fast, and simple method of fabrication to provide high homogeneity in the NP distribution as well as good reproducibility in their properties. Sol–gel process as a typical chemical method provides an attractive route for the preparation of multicomponent oxide materials assuring homogeneity in the deposition of the film on the substrate. In this work, SPR has been explored as optical transduction technique for monitoring the response of TiO_2 thin films doped with Au-NPs prepared by the sol–gel method as sensing layers for H_2 and CO. The nanocomposite thin films were investigated from both optical and morphological points of view. The application of the TiO_2–Au films as optical sensing materials has been evaluated by detecting the changes in the optical absorption spectra upon exposure to different concentration gases. In addition, the cross selectivity is also calculated and discussed.

For synthesizing gold-containing TiO_2 sol (0.1 Au/Ti atomic ratio), a pure oxide sol and a solution of Au^{3+} ion was separately prepared. The Au^{3+} precursor was hydrogen tetrachloroaurate (III) hydrate ($HAuCl_4 \cdot 3H_2O$).[20] A suitable ligand for the formation of metal ion complexes was introduced in the $HAuCl_4 \cdot 3H_2O$ solution, which was then poured into the oxide sol under stirring. For preparing Au^{3+}-doped TiO_2 sols, tetrahydrofuran (C_4H_8O (THF)) was used as a solvent, and the reactants was in the following molar ratios: $Ti(OC_4H_9)_4$:THF:H_2O:acacH = 1:5:4:0.8.[21] The Ti precursor was first chelated with acacH dissolved in 1-butanol and the resulting solution was stirred for 1 h. Then the required amount of water dissolved in 2-propanol was added for hydrolyzing the Ti precursor and the sol was stirred for 1 h before adding the metal-containing solution. The resulting sol was further stirred for 1 h.

For the deposition of coatings, fused silica or glass substrates were cleaned in 2-propanol and in concentrated hydrochloric acid, then rinsed in deionized water. Coatings were deposited onto the cleaned substrates by spin coating, with a spinning rate of 3500 rpm for 25 s. The spinning apparatus was put in a portable glove box, in which a nitrogen flow was kept at a constant RH value of 35% during the whole spinning operation.

After spinning, a continuous and slow cooling process was chosen to perform the annealing treatment. The films were dried for 10 min at 80 °C in air, then, underwent thermal annealing in a tube furnace at temperatures progressively increasing from 100 to 500 °C, with a temperature gradient of 200 °C h^{-1}. In this case the films were directly heated to the desired temperature without any standing at lower temperatures.

The surface morphology was observed an atomic force microscope (CSPM4000) in contact mode. Optical absorption spectra of samples were acquired on CARY 500 Scan UV-vis-NIR Spectrophotometer. The crystallographic properties of the composite films were analyzed by X-ray diffraction (XRD, Philips, X-Pert MRD) using a monochromatized Cu Kα in the θ_0–2θ thin film configuration, where θ_0 was fixed at 0.5°.

Figures 1(a) and (b) show AFM scanning images of TiO_2 films prepared with inclusions of Au-NPs at annealing temperature of 300 °C (sample A) and 500 °C (sample B), respectively. The AFM images reveal that Au NPs of smaller size can be obtained with lower annealing temperature. At annealing temperature of 500 °C (Fig. 1(b)), the average size of the NP is determined to be 33 nm. The average height is found about half of the diameter (15.5 nm), indicative of a hemispherical shape.

Absorption spectra of TiO_2–Au films for samples heated at 300 °C and 500 °C are reported in Figure 2. The SPR band resulting from the gold nanoparticles in TiO_2–Au films is clearly visible in each film. This absorption band agrees with previous observations of the LSPR spectrum of Au NPs.[22] The frequency of the plasmon band undergoes a red-shift at increasing annealing temperature, the dependence of this shift on the embedding medium indicates the high sensitivity of surface plasmon band to cluster-matrix interface properties. This fact is originated to the increase

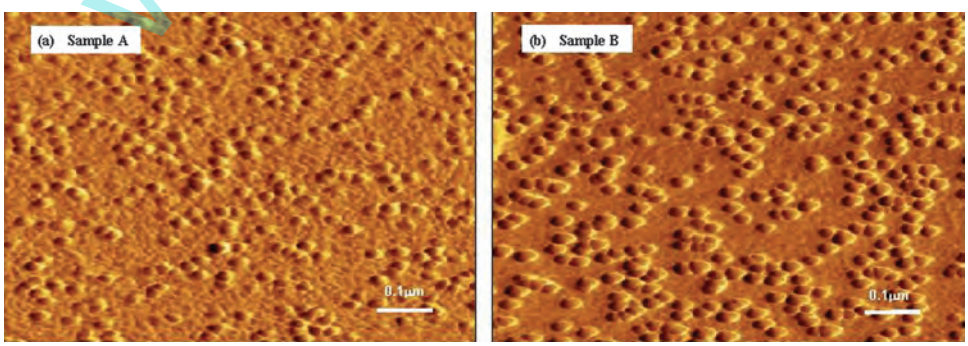

Fig. 1. AFM images of Au–TiO_2 nanocomposite films after annealing at 300 and 500 °C. Sample A (300 °C), Sample B (500 °C).

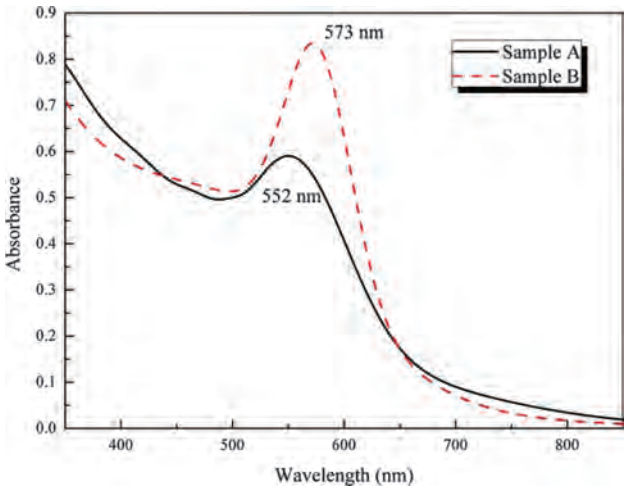

Fig. 2. Optical absorption spectra of Au–TiO_2 nanocomposite films after annealing at 300 and 500 °C.

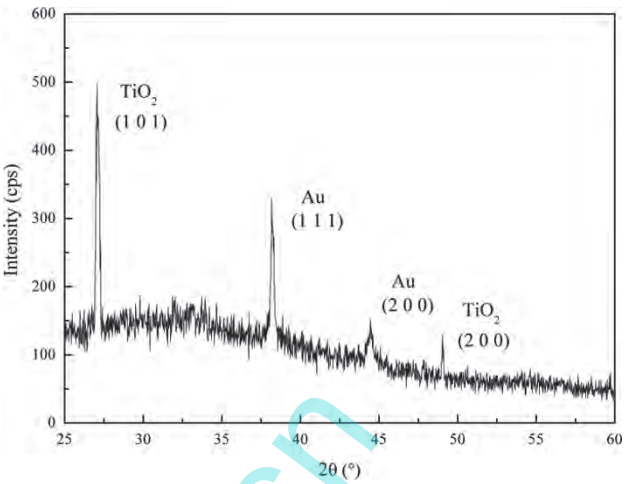

Fig. 4. XRD pattern of Au–TiO_2 nanocomposite thin film annealed at 500 °C.

in the diameter of Au nanoparticles and an increment of the refractive index of TiO_2 matrix with increasing the heat-treatment temperature.[23, 24]

Figure 3 shows the results of the average size (diameter) of the gold particles in the nanocomposite films. The values of Au NPs (clusters) size range from about 12 nm at 100 °C to approximately 33 nm at 500 °C. In accordance to the results, the Au particles are confined on the nanometrical scale, which growth led by the diffusion of the Au atoms, promoted by the annealing treatments. The SPR activity and the related changes on the optical properties are directly affected by this growth. Figure 3 clearly illustrates a continuous increase of the Au particles size in this temperature range. Film thicknesses for TiO_2–Au films at different annealing temperatures are measured using ellipsometry. The thickness of the TiO_2–Au films annealed at 300 and 500 °C are 51 nm and 45 nm, respectively.

The XRD pattern of deposited TiO_2–Au thin film is shown in Figure 4 that show the micro-structural composition of TiO_2–Au film annealed up to 500 °C. The detectable peaks arise from (111) and (2 0 0) planes of the cubic lattice of crystalline metal gold (powder diffraction file no. 04-0784, International Centre for Diffraction Data (ICDD), Newton Square, PA). When annealing at 500 °C, TiO_2 matrix assumes the anatase crystalline structure, as evident from the (101) and (2 0 0) anatase diffraction peaks (powder diffraction file no. 86-1157, ICCD).

Figure 5 illustrates the absorbance spectrum of Au–TiO_2 nanocomposite for different gas flow at 23 °C under a relative humidity (RH) of 30%. In both cases the introduction of gaseous environment within the sample chamber provokes a marked decrease of the SPR band absorbance level, as well as a noticeable increase of the resonance frequency visualized as a blue shift of the SPR wavelength. Without any targeted gas the SPR peak was at 573 nm, while with 2% H_2 exposure the peak rises at 566 nm, and

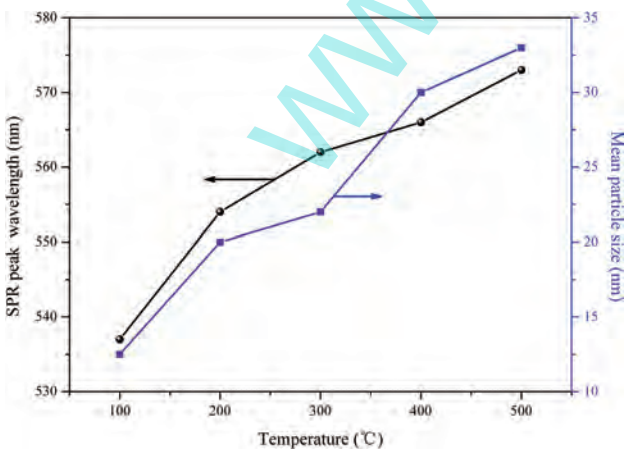

Fig. 3. The measured SPR peak wavelength and mean particle size at different annealing temperatures.

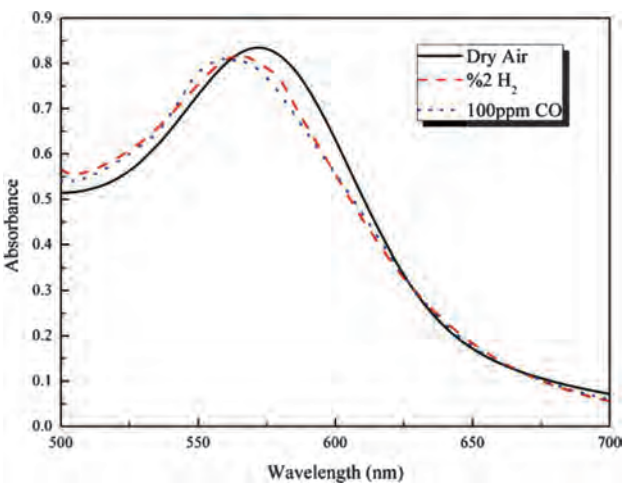

Fig. 5. Absorption spectra of Au–TiO_2 films exposed to dry air, H_2 and CO.

with 100 ppm CO the SPR peak is obtained at 564 nm. Subsequently, all sensing measurements will be conducted at this working condition.

The data demonstrate that the nature of the interaction of the sample with the target gas is directly affecting the dielectric medium surrounding the Au-NPs. According to the Mie theory, the SPR wavelength is:

$$\lambda_{\text{peak}} = 2\pi c\sqrt{\frac{m\varepsilon_0}{Ne^2}(\varepsilon_\infty + 2\varepsilon_m)} \quad (1)$$

where ε_∞ is the high-frequency dielectric constant of Au, ε_m is the dielectric constant of the medium, N is the electron concentration, m the effective mass of conduction electrons, ε_0 is the vacuum permittivity, e is the electron charge, and c is the velocity of light. The chemical interaction of the H_2 and CO molecules on the Au surface or on ites vicinity will increase the overall electron concentration on the metal side. The transfer of electrons from the gases to Au nanocrystals cause a change in the SPR resonant wavelength. In the sol–gel method, the nanoparticles are formed into the matrix films, not formed on the films. Therefore, in this study, the particles exist half buried, and their shape are hemispherical and the absorption spectrum depend on the shape of NPs which is different from the calculated result using Eq. (1).

In this work the gas sensor signal is defined as the percent change in SPR peak shift in absence and presence of the target gas $|\lambda_{\text{gas}} - \lambda_{\text{no gas}}|/\lambda_{\text{no gas}} \times 100$. Here λ_{gas} and $\lambda_{\text{no gas}}$ indicate wavelengths where the SPR peak was observed for the Au–TiO_2 films in absence and presence of the target gas respectively. Sensing response toward the variation of gases based on the change of the LSPR spectra, i.e., the shift of resonance peak positions. Variations of gas sensor signal with concentration of H_2 and CO are shown in Figure 6. The plots provide further evidence of the higher sensitivity of the films toward detection of CO. The intensity of the optical response is proportional to the order of magnitude of the target gas concentration. Since the relationship is linear, calibration curves are extremely easy to set, as shown in Figure 6.

Under the normal conditions, a gas sensor detects the presence of a particular gas. However, it is very important to evaluate the ability of a sensor to respond to a specific gas exposure while another gas is present at a low concentration. In this study we introduce H_2 while exposing the sensing gold film at the exposure of CO to determine the cross selectivity. The following expression was used to do the calculations:

$$\text{Cross selectivity} = \frac{|\lambda_{H_2} - \lambda_{CO}|}{\lambda_{H_2}} \times 100 \quad (2)$$

Where λ_{H_2} and λ_{CO} represent the SPR peaks observed for the Au–TiO_2 films in presence of 10% H_2 and CO with various concentrations. The Au–TiO_2 films based sensors were tested for their cross selectivity for CO in presence of H_2 gas. For this purpose the absorption spectra with SPR peak at 550 nm was recorded in presence of 10% H_2. Later, in the same H_2 environment, CO was introduced in various concentrations. The change in absorption spectra with SPR peak shift is recorded, and the result is given in Figure 7.

On decorating the Au-NPs at the room temperature gas adsorption can be made possible due to the presence of Au on the surface. Ionsorption of oxygen ions can occur on Au-NP surface at room temperature due to the highly conductive nature and availability of free electron in Au. The conductive NP thereafter spills the gas over semiconductor surface via spillover effect.[25, 26] The spillover effect via catalytic activation due to gold nanoparticle and chemical sensitization is observed to be responsible for room temperature H_2 and CO sensing.

In conclusion, Au-NPs embedded TiO_2 film was synthesized by sol–gel method. The films have been characterized using AFM, XRD and optical absorption spectra. The occurrence LSPR depends on morphology

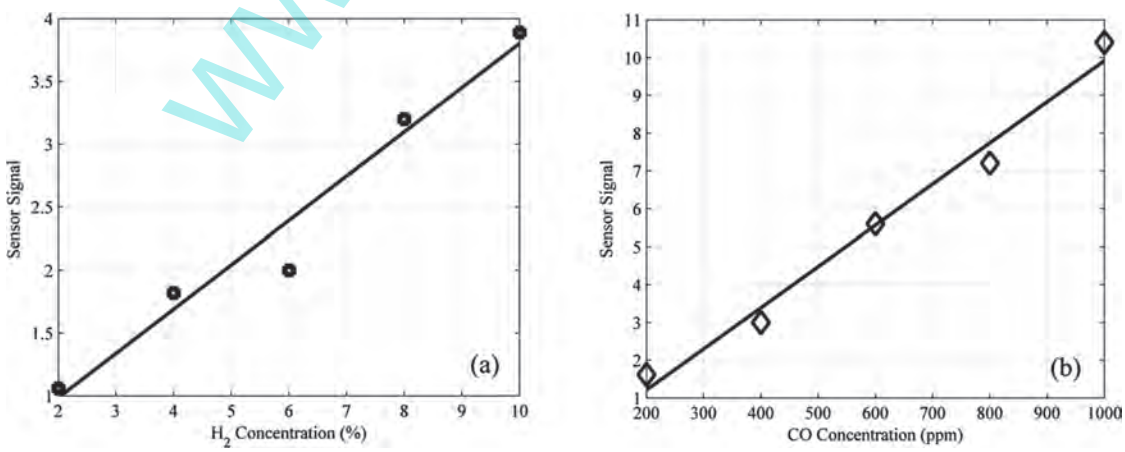

Fig. 6. Variation of gas sensor signal with H_2 (a) and CO (b) gas concentration for Au–TiO_2 films at 23 °C.

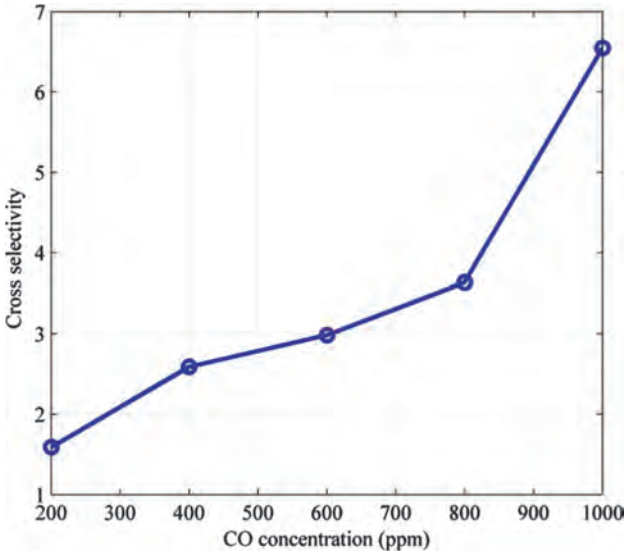

Fig. 7. Cross selectivity of Au–TiO_2 film for CO in presence of 10% H_2.

and the nature of the sensing materials and it is considered as a predominant phenomenon in our Au–TiO_2 composite films. The investigation shows that the LSPR is sensitive toward the presence of target gases. The sensing parameter is based on changing the resonant peak wavelength and its intensity showed a linear relationship with the gas concentration. Metal nanoparticles act as catalyst in chemical sensitization and can improve the sensing characteristics. This study shows the applicability of Au-NPs as catalyst for gas sensor applications.

Acknowledgments: Project supported by the National Natural Science Foundation of China (Grants Nos. 61203211, 20907021) and the Foundation for Outstanding Young Teachers of Nanjing University of Information Science and Technology (No. 20110423).

References and Notes

1. S. A. Maier, Plasmonics: Fundamentals and Applications, Springer, New York (**2007**).
2. K. S. Binpin and C. H. Andrew, *Anal. Chem.* 78, 2009 (**2006**).
3. J. Rao and R. J. Winfield, *Sensor Lett.* 8, 378 (**2010**).
4. G. A. Niklasson, C. G. Granqvist, and O. Hunderi, *Appl. Opt.* 20, 26 (**1981**).
5. D. Kohl, *Sens. Actuators B* 1, 158 (**1990**).
6. E.D.Gaspera, M. Guglielmi, S. Agnoli, G. Granozzi, M. L. Post, V. Bello, G. Mattei, and A. Martucci, *Chem. Mater.* 22, 3407 (**2010**).
7. G. Walters and I. P. Parkin, *J. Mater. Chem.* 19, 574 (**2009**).
8. Y. W. Fen, W.-M. M. Yunus, and N. A. Yusof, *Sensor Lett.* 9, 1704 (**2011**).
9. R. Gradess, R. Abargues, A. Habbou, J. C. Ferrer, E. Pedrueza, A. Russell, J. L. Valdés, and J. P. Martínez-Pastor, *J. Mater. Chem.* 19, 9233 (**2009**).
10. Y. S. Sohn, *Sensor Lett.* 9, 272 (**2011**).
11. H. Li and P. Wei, *Sensor Lett.* 10, 1566 (**2012**).
12. M. H. Seo, M. Yuasa, T. Kida, J. S. Huh, K. Shimanoe, and N. Yamazoe, *Sens. Actuators B* 137, 513 (**2009**).
13. Z. M. Seeley, A. Bandyopadhyay, and S. Bose, *Thin Solid Films* 519, 434 (**2010**).
14. Z. Wang, L. Shi, F. Wu, S. Yuan, Y. Zhao, and M. Zhang, *Nanotechnology* 22, 275502 (**2011**).
15. I. Bannat, K. Wessels, T. Oekermann, J. Rathousky, D. Bahnemann, and M. Wark, *Chem. Mater.* 21, 1645 (**2009**).
16. M. Haruta, *Catal. Today* 36, 153 (**1997**).
17. D. T. Thompson, *Top. Catal.* 38, 231 (**2006**).
18. P. Mulvaney, *Langmuir* 12, 788 (**1996**).
19. A. Siozios, D. C. Koutsogeorgis, E. Lidorikis, G. P. Dimitrakopulos, T. Kehagias, H. Zoubos, P. Komninou, W. M. Cranton, C. Kosmidis, and P. Patsalas, *Nano Lett.* 12, 259 (**2011**).
20. M. G. Manera, J. Spadavecchia, D. Buso, F. C. Julián, G. Mattei, A. Martucci, P. Mulvaney, J. Pérez-Juste, R. Rella, L. Vasanelli, and P. Mazzoldi, *Sensor Actuat. B* 132, 107 (**2008**).
21. M. Epifani, C. Giannini, L. Tapfer, and L. Vasanelli, *J. Am. Ceram. Soc.* 83, 2385 (**2000**).
22. B. Sepúlveda, P. C. Angelomé, L. M. Lechuga, and L. M. Liz-Marzán, *Nano Today* 4, 244 (**2009**).
23. S. Underwood and P. Mulvaney, *Langmuir* 10, 3427 (**1994**).
24. A. Ito, H. Masumoto, and T. Goto, *Mater. Trans.* 44, 1599 (**2003**).
25. R. K. Joshi and F. E. Kuris, *Appl. Phys. Lett.* 89, 153116 (**2006**).
26. R. K. Joshi, Q. Hu, F. Alvi, N. Joshi, and A. Kumar, *J. Phys. Chem. C* 113, 16199 (**2009**).